Eur. Phys. J. B **10**, 543–548 (1999)

THE EUROPEAN PHYSICAL JOURNAL B

EDP Sciences

A nonlinear model for aeolian sand ripples

A. Valance[a] and F. Rioual

Groupe Matière Condensée et Matériaux[b], Université Rennes 1, 35042 Rennes Cedex, France

Received 5 January 1999

Abstract. Starting from the phenomenological model for sand ripple formation developed in [1], we proposed a new interpretation in the light of recent experiments. Furthermore, we derive, close to the threshold of ripple instability, a nonlinear equation for the spatio-temporal evolution of the sand bed profile, which to leading order has a quadratic nonlinearity. This equation is identical to that derived recently on the basis of geometry and conservation law [2]. Our derivation connects the coefficients of the nonlinear equation to the underlying physical mechanisms (reptation length...). This equation reveals ripple structures which then undergo a coarsening process, as observed in wind tunnel experiment. Small, fast moving ripples are absorbed by larger, slower forms resulting in a growth of the mean wavelength.

PACS. 83.70.Fn Granular solids – 81.05.Rm Porous materials; granular materials – 47.20.-k Hydrodynamic stability

1 Introduction

A flat sand surface, when subjected to moving air, is usually unstable and gives rise to fascinating regular patterns resembling surface waves. These patterns can be classified into two distinct structures differing by their length scale: ripples (small structures) and dunes (large ones). Here, we shall focus on the formation and dynamics of the smaller class of bedforms, that are the ripples. Although these patterns are commonly observed in nature (like in deserts or coastal regions), no general theory exists for the complex interaction of wind and sand grains responsible for the formation of aeolian ripples.

The study of aeolian ripples has been largely guided by Bagnold's seminal work [3]. We find it worthwhile recalling the main outcomes of Bagnold about the process of aeolian sand transport. The aeolian sand transport can be described in terms of a cloud of grains leaping along the sand surface. According to Bagnold [3], there are two distinct modes of transport: (i) saltation and (ii) reptation (or surface creep using the terminology of Bagnold)[1] (i) The saltating grains are those capable of rebounding or splashing up other grains. One can think of saltating grains as the high-energy subpopulation of the grains in motion. These grains regain from the wind the energy lost when rebounding and can therefore travel over long distances. Their trajectory in the air is determined by several intricate parameters such as the wind velocity profile, air friction and initial energy of the grain when it leaves the sand bed. Bagnold identified a characteristic path length in saltation. One of the salient features is the flat incident angle which ranges from 10° to 15°. (ii) The reptating grains represent the low-energy grains. They are ejected from the bed under the impact of the saltating grains and have relatively short and low trajectories so that they can not regain energy from the wind.

Bagnold work on aeolian transport has been refined by subsequent workers. Recent experiments [4,5] and numerical simulations [6–8] have focused on the coupling between saltation impacts and surface grain motion (*i.e.*, reptation). They report that the bed impact of one saltating grain typically results in one energetic ricocheted grain and a large number of emergent grains (*i.e.*, low-energy ejecta). The ricocheted grain leaves the surface with roughly two-third of the impact velocity while the emergent grains have a mean ejection speed less than 10 per cent of the impact speed and therefore have a short trajectory.

Other works [9] have focused on the modification of the wind profile within the saltation curtain. It was found that during steady-state saltation, the aerodynamic stress at the bed is reduced to below that necessary to entrain grains from the bed. This important result, already mentioned by Bagnold, has led to the following major conclusion: although aeolian saltation is initiated by aerodynamic forces, the maintenance of saltation relies essentially through impacts. In other words, the ejection of grains from sand bed is essentially induced by the impact of saltating grains.

Starting from the knowledge of saltating transport, several authors attempt to elaborate a theory in order to explain the formation of aeolian ripples. The first

[a] e-mail: `valance@truffaut.univ-rennes1.fr`

[b] UMR 6626

[1] One should also add a third mode of transport which is suspension and concerns only very small grains.

explanation was proposed by Bagnold [3]. He argued that the spatial variation of the reptating flux is responsible for the growth of ripples. Indeed, he put forward the idea that the mass flux of reptating grains at any point of the surface is proportional to the flux of saltating grains impacting the sand bed at that point. If a small deformation of the surface occurs, the windward slope will be more exposed to the incoming saltating grains than the lee side. A greater number of reptating grains will therefore be driven up to the stoss slope (through reptation motion) than down to the reverse slope. As a result, the deformation will grow. Bagnold moreover pointed to a close correspondence between saltation path lengths and ripple spacing. A more quantitative analytical model has been proposed by Anderson [10] which describes more precisely the coupling between the saltation impacts and the surface grain motion (*i.e.*, reptation). Such a model predicts that a flat surface is unstable in favour of ripple structure. The fastest growing mode, which is expected to give the wavelength of the ripple, is found to be of order of several times the mean reptation length, in contradiction with Bagnold vision. This analytical model has been refined later on by Hoyle [11].

Numerous numerical models [12,13] have been also developed. Anderson [12] built his own numerical model confirming the prediction of his analytical model and suggesting that the ripple wavelength increases in course of time (the final spacing can be several times larger than the initial one) which is consistent with the experiments [12]. Nishimori *et al.* [13] proposed a model where the saltation length varies according to which height the saltating grain has taken off. They find a ripple pattern whose wavelength is proportional to the mean saltation length but can not account for the evolution of the ripple spacing in course of time.

The purpose of the present contribution is to extend Anderson model [10] (which to our mind is the most faithful to experimental facts) to account for the nonlinear development of the sand bed structure after the initiation of the ripple instability. Anderson analysis is based on a linear stability analysis which is expected to be valid only in the first stages of the instability initiation and can not predict the evolution of the ripple pattern neither the final morphology, wavelength and velocity of the structure. Starting from the phenomenological model developed in [1] which is based on the description of the coupling between grains at rest and grains in motion, we derive a nonlinear equation for the evolution of the sand bed profile close to the ripple instability threshold. This equation takes the simple following canonical form

$$h_t = -\partial_x^2 h - \partial_x^4 h + \nu \partial_x^3 h + \partial_x^2[(\partial_x h)^2] \qquad (1)$$

where $h(x,t)$ measures the height of the sand bed profile. As to be seen below, this equation can always be reduced to an equation with only one dimensionless parameter denoted ν. It has been shown [2] that this ripple equation can be obtained simply from general considerations based on geometry and conservation. In particular, the nonlinear term of equation (1) can be directly inferred from mass conservation. Of course, this is not the only nonlinear term compatible with mass conservation but it turns out to be the leading nonlinear contribution. One can note also that this equation differs from that proposed by Hoyle [11]. Indeed, in the Hoyle model the nonlinear contribution is of the form $[1-(\partial_x h)^2]^{-3/2}\partial_{xx} h$ (with $\partial_x h \sim 1$). This nonlinear contribution is inferred to avalanche process that we do not believe to be pertinent in the formation of aeolian ripples.

In this paper, we derive equation (1) from a physical model which allows us to evaluate precisely the coefficients of each term appearing in the equation but also to relate them to the underlying physical mechanisms. This nonlinear equation reveals ripple structures which undergo a corseaning process, as studied in [2]. This coarsening process can be easily interpreted in terms of ripple coalescence and seems to be fully consistent with observations in wind tunnel experiments [12].

The paper is organized as follows. In the second section, we recall the view adopted for describing the saltation process and present our model inspired from that proposed by Anderson. Section 3 is devoted to the stability analysis of a flat sand bed exposed to a stationary saltation process while in Section 4 we derive a nonlinear equation for the subsequent spatio-temporal evolution of the ripple pattern. Conclusion and prospects are given in the last section.

2 Model

The view adopted here to describe the saltation process conforms with that of most previous studies in that the motion of grains comprising aeolian ripple is believed to result not directly from fluid forces imposed by the air but rather from the impact of saltating grains that are themselves accelerated by the wind. Although aeolian saltation must be initiated by aerodynamic forces, it is the subsequent impacts of saltating grains that appear to be responsible for most of the ejection of grains into the airstream during fully developed saltation.

The phenomenological approach we consider is the same as that developed in [1]. It is based on the description of the interaction between the moving grains (*i.e.*, saltating and reptating grains) and the grains at rest in sand bed. Unlike the model in [1], we find more realistic, according the previous studies on saltation, to distinguish two types of moving grains, that is the saltating grains of long high-energy trajectories and the low-energy splashed grains travelling in reptation. This distinction will allow us to relate easily the phenomenological coefficient introduced in our model with the observed phenomena. The impact of saltating grains can be seen as the driving force which governs the motion of surface participating in aeolian ripple growth and translation. In the so-called fully developed saltation, erosion is counterbalanced by deposition and the population of saltating grains is almost constant. In essence, we assume that the saltating grains have zero probability of death during impact: it reproduces itself perfectly. The saltating grains can be considered just

as spectators (the saltating population does not exchange grains with the reptating population) which serve only to bring energy into the system. Therefore, we will only consider an exchange of grains between the reptating grains and the grains at rest. We call the reptating grains density $R(x,t)$ where x is the coordinate in the direction of the wind and t the time. It will assume here that the system is translationally invariant in the direction transverse to the wind. The grains at rest are measured in terms of the local height $h(x,t)$ of the static bed. In the thermodynamical limit, the dynamical equations of h and R read

$$\partial_t R = -V\partial_x(R) + \Gamma[R,h] \tag{2}$$

$$\partial_t h = -\Gamma[R,h] \tag{3}$$

where V the mean velocity of the reptating grains in the wind direction.

Γ describes the exchange rate between the reptating grains and the grains at rest and depends *a priori* on R and h. In comparison with the model in [1], we omit the diffusion term in the first equation, which is not pertinent for our purpose, as to be seen further below. Note that R has been defined such that it has the same dimension as h (R can be thought as the width of grains which have been removed from the static bed).

We should write now the expression for Γ by using phenomenological physical arguments. Γ can be split into two terms, one describing the deposition process of the reptating grains and the other modelling the ejection of the reptating grains under the impact of the saltating grains and occasionally under the wind force: $\Gamma = \Gamma_{\rm dep} + \Gamma_{\rm ej}$.

(i) We have seen that the ejection of grains in steady-state saltation is essentially due to impacts. The rate of ejection should therefore largely depend on the flux of saltating grains impacting the sand bed. In a smaller extent, one can also expect that a small part of the reptating grains are set in motion thanks to the wind force. The flux of saltating grains impacting the sand bed at one point is dependent on the local orientation of the sand surface at that point with respect to the incidence direction of the impacting grains. In addition, it is reasonable to think of that the efficiency of ejection mechanism is sensitive to the local curvature of the sand surface: grains are harder to dislodge upon impact in troughs than at the top a crest. Identically, the direct entrainment of grains by the wind should be *a priori* dependent on the local slope and curvature of the bed profile. One can thus write:

$$\Gamma_{\rm ej} = \Gamma^{\rm a}_{\rm ej} + \Gamma^{\rm b}_{\rm ej} \tag{4}$$

with

$$\Gamma^{\rm a}_{\rm ej} = \alpha_0(1 + \alpha_1\partial_x h - \alpha_2\partial_x^2 h), \tag{5}$$

$$\Gamma^{\rm b}_{\rm ej} = \beta_0(1 + \beta_1\partial_x h - \beta_2\partial_x^2 h), \tag{6}$$

where α_i and β_i are constant and positive coefficients . (The wind has been assumed to blow in the same direction as the oriented axis $(0x)$). α_0 is proportional to the flux of the saltating grains and β_0 to the wind force.

The coefficients α_0 and α_1 can be simply deduced from the features of the saltating grains. According to Bagnold observations [3], the incident angle of impacting grains appears to remain remarkably constant. The saltating grains can thus be seen as a rain of sand grains impacting the surface with a constant angle. Assuming that the number N of ejected grains per unit time from the surface at position x is proportional to the flux of saltating grains perpendicular to the surface at that point, we get

$$N \simeq nd^2 J\tan\theta(1 + \cot\theta\partial_x h) \tag{7}$$

where n is the number of grains ejected per saltating grain, d is the diameter of the grains, J is the saltation flux and θ the angle of incidence with respect to the horizontal. From that expression, we directly deduce that $\alpha_0 = nd^3 J\tan\theta$ and $\alpha_1 = \cot\theta$. The estimation of the coefficient α_2 which reflects curvature effect is more delicate but it can be in principle also measured through appropriate experiments.

The coefficients β_i are related to the wind force. Usually, as seen before, the direct dislodgement of the surface grains by the wind is weak because the wind is screened by the saltating grains. Indeed, it has been found from simulations [9,10] that the fluid entrainment is unimportant for flat surface. However, we think that the direct dislodgement by the wind of a grain located on the top of a bump should be a significant process (as a tip effect in electrostatic). The wind, even if it is weak, tends to smooth a surface made of grains. As a consequence, we expect that the wind entrainment is essentially dominated by the curvature effect: $\Gamma^{\rm b}_{\rm ej} \simeq -\beta\partial_x^2 h$ where $\beta = \beta_0\beta_2$.

(ii) The deposition process concerns only the reptating grains. We will assume that the rate of deposition at point x is proportional to the number R of reptating grains at that point[2] so that we can write

$$\Gamma_{\rm dep} = -R\gamma \tag{8}$$

where γ^{-1} represents the typical time during which the reptating grains are moving before being incorporated to the sand bed. This life time can be interpreted in terms of the characteristic reptation length l which can be defined by $l = V/\gamma$ where V is the mean speed of the reptating grains along the wind direction. l is a quantity which can be evaluated from experiments. Given the energy and the incident angle of the saltating grains, l can be measured as a function of the topography of the sand bed (*i.e.*, the local slope and curvature of the bed profile). This is precisely the purpose of a new experiment carried out in the Bideau group [15]. One expect *a priori* that l should be larger on a slope facing the wind (a reptating grain on a stoss face can gain an additional energy from the wind) than on a lee slope. Using the same intuition, we can also argue that the reptation length is again larger on the top of a crest that in a through. These two effects can be modelled as follows through the life time γ^{-1}

$$\gamma = \gamma_0(1 - \gamma_1\partial_x h + \gamma_2\partial_x^2 h). \tag{9}$$

[2] One assumes implicitly here that the deposition process is a local one. It is justified if the characteristic lengthscale of interaction (which is here the reptation length as to be seen below) is smaller than the wavelength of the ripple structure. This is generally the case for aeolian sand ripples.

where the coefficients γ_i are taken to be positive. γ_0^{-1} is nothing but the life time for the reptating grains moving on a sand flat surface. As to be seen later on, the sign of γ_1 is very important because it determines the sign of the nonlinear term in the equation (1) for the sand bed profile evolution and therefore the shape of the ripple.

In the light of the previous considerations, we will assume Γ to be of the following form

$$\Gamma = \alpha_0(1 + \alpha_1\partial_x h + \alpha_2\partial_x^2 h) + \beta\partial_x^2 h - R\gamma_0(1 - \gamma_1\partial_x h + \gamma_2\partial_x^2 h). \quad (10)$$

The set of equations (2, 3, 10) describes completely our system. Note that these equations are nonlinear and non trivial dynamics is expected. Some essential features of the model can be first investigated by linearizing the system in the vicinity of the situation where the sand bed is flat ($h = h_0$). In this case, the density of the reptating grains is simply given by setting $\Gamma = 0$ which yields $R_0 = \alpha_0/\gamma_0$.

3 Linear stability analysis

We present here briefly the linear stability analysis of a flat sand bed. We consider small perturbations of R and h

$$R = R_0 + R_1 \quad (11)$$
$$h = h_0 + h_1 \quad (12)$$

where h_1 and R_1 are of the form $\mathrm{e}^{\mathrm{i}kx+\Omega t}$ (k is the wave number of the perturbation and Ω its growth rate). Plugging equations (11, 12) into the motion equations and neglecting the nonlinear terms, we get a compatibility condition which yields

$$\Omega = -\gamma_0 l_0 \mathrm{i}k \frac{l_0 R_0(\alpha_1+\gamma_1)\mathrm{i}k + l_0 R_0(\alpha_2+\gamma_2)k^2 - (\beta/\gamma_0)k^2}{1 + l_0\mathrm{i}k} \quad (13)$$

where $l_0 = V/\gamma_0$ stands for the characteristic reptation length for a flat surface. It is a simple matter to show that the most dangerous modes are those of longwavelength (as compared to the reptation length). Therefore we expect the nonlinear behaviour close to the threshold of ripple formation to be dominated by these modes. In the limit of longwavelength perturbation, the growth rate simply reads

$$\frac{\Omega}{\gamma_0} \simeq \varepsilon(\alpha_1+\gamma_1)l_0^2k^2 - \varepsilon l_0^2[(\alpha_2+\gamma_2) + (\alpha_1+\gamma_1)l_0](\mathrm{i}k^3 + l_0k^4) - l_0(\beta/\gamma_0)(\mathrm{i}k^3 + l_0k^4) \quad (14)$$

where $\varepsilon = \alpha_0/V$. It can be seen that at small k, the sign of Ω is determined by that of the coefficient of the quadratic term. As $(\alpha_1 + \gamma_1)\varepsilon$ is positive, the flat sand surface is always unstable. There exist a band of unstable wave vectors ranging from 0 to a cut-off k_c (see Fig. 1). However, in the particular case where $\varepsilon = 0$ (*i.e.*, $\alpha_0 = 0$; it means that the wind is too weak to maintain saltation), the surface is marginally stable.

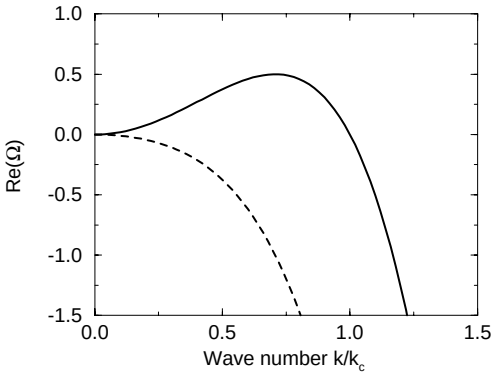

Fig. 1. Real part of the growth rate as a function of the wave number. Full line: unstable. Dashed line: marginal stability.

We can examine the case close the instability threshold (*i.e.*, $\varepsilon \ll 1$). We will see later on that ε turns out to be smaller than unity for standard conditions of saltation. In this limit, we simply have

$$\mathrm{Re}(\Omega) \simeq \gamma_0\left[\varepsilon(\alpha_1+\gamma_1)l_0^2k^2 - l_0^3 l_c k^4\right] \quad (15)$$
$$\mathrm{Im}(\Omega) \simeq \gamma_0 l_0^2 l_c k^3 \quad (16)$$

where we have set $l_c = \beta/V$. l_c has the dimension of a length and plays the role of a cut-off length which prevents the surface from arbitrary small deformations. Indeed, l_c appears as the prefactor of the quartic term of equation (15) which dominates at short wavelengths and therefore stabilizes the structure. l_c can be seen as the shortest length of deformation of the surface. We can easily evaluate the most dangerous mode $k_{\max}$ (that is the mode which has the fastest growth rate). The wavelength of the most dangerous mode is found to be

$$\lambda_{\max} = \frac{2\pi}{k_{\max}} = 2\pi\frac{\sqrt{2l_0l_c}}{\sqrt{\varepsilon(\alpha_1+\gamma_1)}}\cdot \quad (17)$$

One can note that the most dangerous mode which is expected to dominate the subsequent evolution of the pattern is given by the geometrical average between the reptation length l_0 and l_c. (One should also point out that this result is different from that in [1] where the wavelength of the most dangerous mode is found to be of order of the mean hopping length defined as the average between the long jumps of the saltating grains and the short jumps of the reptating grains. Let us try here to estimate $\lambda_{\max}$. The estimation of the order of magnitude of l_c is not trivial. However, it is the smallest lengthscale of our problem. So, if we assume that l_c is at least ten times smaller than the reptation length l_0, $\lambda_{\max} \sim 6l_0$ for $\varepsilon \simeq 0.1$ which seems reasonable.

Finally, the non-zero imaginary part of the growth rate indicates that the unstable modes propagate along the sand surface. The propagation speed of the modes k is simply given by $V_d = -\mathrm{Im}(\Omega)/k$. For the most dangerous

mode, we get

$$V_{\rm d} = \frac{\varepsilon}{2}(\alpha_1 + \gamma_1)V. \tag{18}$$

Two remarks are in order. First, one can note that the ripples propagate in the same direction as the wind. Second, according to experimental observations [3], the propagation speed of the ripples is much smaller than the velocity of the surface grains (*i.e.*, reptating grains). One can therefore conclude that the assumption $\varepsilon \ll 1$ is justified.

4 Nonlinear analysis

In order to investigate the subsequent development of the instability, the nonlinear terms neglected in the linear analysis should be taken into account. To do this, a nonlinear analysis is needed. By means of a multi-scale analysis, it is possible to perform a nonlinear development in the vicinity of the instability threshold. We have at our disposal a small parameter, that is ε which measures the distance from the instability threshold. We have seen from the linear analysis that the growth rate is given by $\Omega \sim \varepsilon k^2 - k^4 + {\rm i}k^3$. The fastest growing mode corresponds to a wave number which scales as $\sqrt{\varepsilon}$ and the corresponding growth rate scales as ε^2. The imaginary part of Ω would scale as $\varepsilon^{3/2}$ and it dominates in principle. This means that in a multi-scale analysis, we have to introduce a short time associated with the propagation and a long time that determines the time scale of the amplification or attenuation of the instability. The total time is $T = T_1 + T_2$ where $T_1 = \varepsilon^{3/2}t$ is the short time and $T_2 = \varepsilon^2 t$ the long time. We also introduce a slow spatial variable $X = \sqrt{\varepsilon}x$. The strategy is to expand the profile h of the sand surface and the density R of the reptating grains in power of $\varepsilon^{1/2}$

$$h = h_1 + \varepsilon^{1/2}h_2 + \varepsilon h_3 + ..., \tag{19}$$

$$R - R_0 = \varepsilon(R_1 + \varepsilon^{1/2} + ...). \tag{20}$$

We note that the first term in the expansion $R - R_0$ scales as ϵ. This is due to the fact that $(R - R_0) \sim \varepsilon h$ as dictated by the linear analysis.

The scheme is to use the equations (2, 3) to deduce successively high-order contributions in power of ε. The first non-trivial contributions come to order $\varepsilon^{3/2}$.

$$R_1 = -\frac{\beta}{\gamma_0}\partial_X^2 h_1, \tag{21}$$

$$\frac{\partial h_1}{\partial T_1} = l_0\beta\partial_X^3 h_1. \tag{22}$$

To next order, we get

$$R_2 = -\frac{\beta}{\gamma_0}\partial_X^2 h_2 + l_0(\alpha_1 + \gamma_1)\partial_X h_1 + l_0\frac{\beta}{\gamma_0}\partial_X^3 h_1 + \beta\frac{\gamma_1}{2\gamma_0}\partial_X[(\partial_X h)^2], \tag{23}$$

$$\frac{\partial h_1}{\partial T_2} + \frac{\partial h_2}{\partial T_1} = l_0\beta\partial_X^3 h_2 - \gamma_0 l_0^2(\alpha_1 + \gamma_1)\partial_X^2 h_1 - l_0^2\beta\partial_X^4 h_1 + l_0\beta\gamma_1\partial_X^2[(\partial_X h_1)^2]. \tag{24}$$

Combining the above equations and setting $H = h_1 + \varepsilon^{1/2}h_2$ and $\mathcal{R} = R_1 + \varepsilon^{1/2}R_2$, we obtain

$$\mathcal{R} = -\frac{\beta}{\gamma_0}\partial_X^2 H + \varepsilon^{1/2}[l_0(\alpha_1 + \gamma_1)\partial_X H - l_0(\beta/\gamma_0)\partial_X^3 H + \beta(\gamma_1/2\gamma_0)\partial_X(H_X^2)], \tag{25}$$

$$\frac{\partial H}{\partial T} = l_0\beta\partial_X^3 H + \varepsilon^{1/2}[-\gamma_0 l_0^2(\alpha_1 + \gamma_1)\partial_X^2 H - l_0^2\beta\partial_X^4 H + l_0\beta\gamma_1\partial_X^2(H_X^2)]. \tag{26}$$

Equation (26) describes the nonlinear evolution of the sand surface. Let us make a few comments about this equation. (i) Seeking perturbations of the form $h \simeq {\rm e}^{{\rm i}kX + \Omega T}$, we recover the linear spectrum $\Omega = -l_0\beta{\rm i}k^3 + \varepsilon^{1/2}[\gamma_0 l_0^2(\alpha_1 + \gamma_1)k^2 - l_0^2\beta k^4]$ found in the linear stability analysis. (ii) After an appropriate rescaling of the variables H, X and T, only one parameter survives and equation (26) can be written in the canonical form (Eq. (1)). It is important to note that equation (1) has been derived in [2] by evoking only geometry, conservation, and locality (which is justified as long as the dominant length scale is the reptation one). In another paper [14], these authors give a class of nonlinear equations derived from these concepts. They distinguish between situations with and without conservation and anisotropy (due to wind for example). With conservation and anisotropy they obtain equation (1). In the absence of conservation and with anisotropy – on the scale of wavelength of interest – (strong erosion), they show that ripples may be described by another class of equation, known as the Benney equation. (iii) $\partial_x^2(h_x^2)$ is the dominant nonlinearity which appears in our multi-scale analysis. If one pursues the development to higher order, the nonlinearity which comes next is $\partial_x(h_x^2)$. This nonlinearity is intrinsically of smaller order than that found to the dominant order ($\partial_x(h_x^2) \sim \varepsilon^{3/2}$ whereas $\partial_x^2(h_x^2) \sim \varepsilon^2$). However, it turns out that this nonlinearity appears with a coefficient containing the small parameter ε, which removes the apparent contradiction.

Numerical integration of this nonlinear equation reveals an evolution towards a ripple pattern (see Fig. 2). One can note first that the stoss slope (*i.e.*, the one facing the wind) is steeper than the lee slope as observed for aeolian sand ripples. Had the sign of the nonlinear term been negative (*i.e.*, $\gamma_1 < 0$), the stoss slope would have been more gentle than the lee slope contrary to field observations. Indeed, changing the sign of the nonlinear term corresponds to an up-down operation in Figure 2. We recall here that a positive γ_1 means that the reptation length is greater on a slope facing the wind that on a lee slope. Second, one should say that contrary to the impression given by Figure 2, the pattern is not stationary; the ripple spacing evolves in course of time. The wavelength is first close to that of the most dangerous mode. As shown in [2], at long time the structure is found to coarsen producing wider and wider ripples. At longer time, the coarsening slows down dramatically. This work is in progress and an extensive study of the evolution of the ripple pattern (height, wavelength and propagation

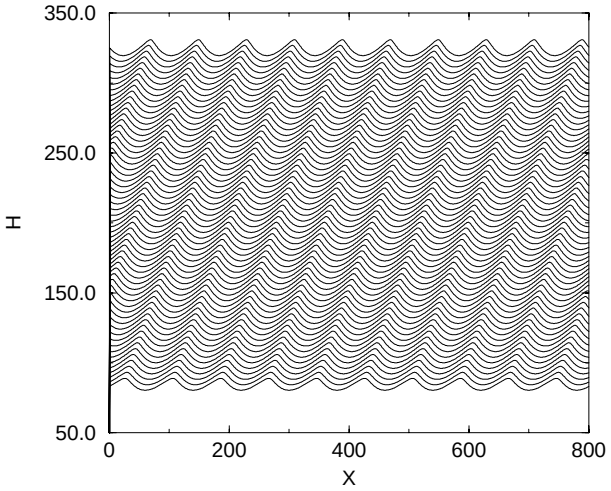

Fig. 2. The ripple profile at different times. The consecutive snapshots have been shifted upward to show the drift.

speed) will be presented in the future. However, we can ascertain that these features agree with field observations and wind tunnel studies [12] which show that the ripple wavelength tends to increase with time by ripple merger, most rapidly at first and slowly thereafter.

5 Conclusion

In summary, we have shown that equations (2, 3) which are phenomenological but motivated by clear physical process allows us to describe the ripple instability as well as its subsequent development. We have derived a nonlinear equation describing the dynamical evolution of a sand surface submitted to wind blow. This equation reveals ripple structures which then undergo a coarsening process as observed in wind tunnel experiments. One task for future is the precise investigation of the evolution of the wavelength, propagation velocity and height of the ripple structure in course of time.

One should also point out the important question about locality of the saltation process. This question arises if the wavelength of the ripple structure is of the same order as the relevant lengthscale of interaction of the problem. In the present study, the interaction between the grains in motion and grains at rest is mediate by the reptating grains. Therefore the characteristic lengthscale of interaction is the reptation length l_0 which is much smaller that the wavelength of the ripple structure [10]. Thus contrary to the believed idea, the formation of aeolian ripple can be treated as a local problem.

Finally, it is worthwhile mentioning open questions. One of the great challenge is to evaluate precisely all the phenomenological parameters of our model from the experiments. This is in principle possible and the recent experiment carried out in Rennes [15] should bring us valuable information about the collision process between impacting grains and static granular bed. It can be also interesting to investigate what happens if one consider two spatial dimensions. Is there an instability corresponding to the transverse meandering of the ripples?

We would like to thank O. Terzidis, P. Claudin and J.-P. Bouchaud for very useful discussions. Through this work, we have also closely interacted with C. Misbah and Z. Csahok.

References

1. O. Terzidis, P. Claudin, J.-P. Bouchaud, Eur. Phys. J. B **5**, 245 (1998).
2. Z. Csahok, C. Misbah, A. Valance, preprint (1998).
3. R.A. Bagnold, *The physics of Blown Sand and Desert Dunes* (Methuen, London, 1941).
4. S. Mitha, M.Q. Tran, B.T. Werner, P.K. Haff, Act. Mech. **63**, 267 (1986).
5. B.B. Willets, M.A. Rice, Act. Mech. **63**, 255 (1986).
6. J. Ungar, P.K. Haff, Sedimentol. **34**, 289 (1987).
7. D.A. Rumpel, Sedimentol. **32**, 267 (1985).
8. B.T. Werner, P.K. Haff, Sedimentol. **35**, 189 (1988).
9. B.T. Werner, J. Geol. **98**, 1 (1990).
10. R.S. Anderson, Sedimentol. **34**, 943 (1987).
11. R.B. Hoyle, A.W. Woods, Phys. Rev. E **56**, 6861 (1997).
12. R.S. Anderson, Earth Sci. Rev. **29**, 77 (1990).
13. H. Nishimori, N. Ouchi, Phys. Rev. Lett. **71**, 197 (1993).
14. Z. Csahok, C. Misbah, A. Valance, Physica D **128**, 87 (1999).
15. F. Rioual, A. Valance, D. Bideau, preprint (1998).